Augmenting Clinical Observations with Visual Features from Longitudinal MRI Data for Improved Dementia Diagnosis*

Devrim Unay
Electrical and Electronics Engineering
Bahcesehir University
Ciragan Cad., Besiktas, 34353
Istanbul, Turkey
devrim.unay@bahcesehir.edu.tr

ABSTRACT

Image-based diagnosis in the medical area often requires qualitative interpretation from the experts, despite the high-resolution of the acquired images. Computation of quantitative measures and comparison of multiple patients using automated medical image analysis tools will help improve the diagnosis and efficiency, especially in the areas such as neurology, where diagnosis from one patient's data has limitations and the prevalence of neurodegenerative diseases is expected to substantially increase in the near future due to the aging population. To this end, this paper presents a novel work on fusing clinical and patient-demographics related observations with visual features computed from brain longitudinal MRI (magnetic resonance imaging) data for improved dementia diagnosis. Experiments with real data showed that augmenting cognitive scores with visual features from a subset of subcortical structures results in more accurate diagnosis. Moreover, subset of structures typically selected are consistent with those (being) investigated in the literature.

Categories and Subject Descriptors

H.3.3 [**Information Storage and Retrieval**]: Information Search and Retrieval; J.3 [**Life and Medical Sciences**]: [medical information systems]; H.2.8 [**Database Management**]: Database Applications—*data mining, image databases*; I.4 [**Image Processing and Computer Vision**]: [Segmentation, Feature Measurement, Image Representation]

General Terms

Experimentation, Performance

Keywords

Automated classification, Dementia Diagnosis, Magnetic Resonance Imaging, Longitudinal analysis, Image processing, Clinical observations, Feature Extraction, Feature Selection

1. INTRODUCTION

Dementia is the loss of cognitive abilities, such as decision making and memory, due to some diseases or conditions affecting the brain. Neurodegeneration, deterioration of brain cells and their interconnections, is one the most common processes underlying dementia. Among many different forms of dementia, Alzheimer's Disease alone accounts for approximately two-thirds of the cases [21]. Age is a risk factor for dementia with about a tenth of people older than 65 being affected, rising to almost half of those over 85. More than 24 million people are estimated to suffer from dementia, worldwide, and this estimate is expected to rise over 80 million by 2040 [4].

Neuroimaging, traditionally used to exclude treatable causes of dementia [19], has become essential for the investigation of patients with dementia over the past few years, due to the increasing need for more accurate diagnosis and prognosis. Accordingly, practice guidelines recommend that neuroimaging should be performed for all dementia cases referred to the neurologist and if available MRI should be preferred over CT and X-Ray [24].

The advances in the medical imaging technology allow for in-vivo visualization and analysis of the human body with unprecedented accuracy and resolution. A diagnosis by a specialist often requires a visit to a radiology department to obtain various images that highlight the suspected pathology. Despite the high resolution of the acquired images, image-based diagnosis often utilizes a considerable amount of qualitative measures. To improve the diagnosis and efficiency, the research in medical image analysis has focused on the computation of quantitative measures by automating some of the error-prone and excruciatingly time-consuming tasks, such as segmentation of a structure.

In image-based diagnosis of dementia, while many researchers explore the binary problem of discrimination between demented and healthy cases, recent research focus has shifted

*This work was supported in part by the Marie Curie Programme of the European Commission under FP7 COSeRMI project PERG05-GA-2009-249253.

MIR'10, March 29–31, 2010, Philadelphia, Pennsylvania, USA.

to identifying 'converters' - the transition group - in order to achieve early diagnosis, improve physical and emotional burden on the patient as well as care-givers, and reduce healthcare costs.

In clinical practice, diagnosis of dementia is generally accomplished by assessing cognitive ability of the subject, investigating demographics and history of the patient, and qualitatively analyzing medical images. Moreover, a promising research field in dementia diagnosis has been to correlate atrophy patterns with cognitive or behavioral performance [14], and identification of atrophy requires processing of longitudinal MRI data. Accordingly, this paper focuses on incorporating cognitive and patient-related observations with visual features (typically those depicting atrophy) automatically computed from brain longitudinal MRI data for the aim of improved dementia diagnosis.

The rest of the paper is organized as follows: Section 2 provides a brief literature review on the topic. Section 3 details the dementia diagnosis method, as well as data and performance evaluation used in this work. Experimental results are presented in Section 4. Finally, the conclusions and the related future works are given in Section 5.

2. RELATED WORK

In the past decade, we have witnessed a rapid growth in the amount of digital media used. This trend has boosted the importance of effective multimedia management and retrieval techniques [12], [18]. Accordingly, content-based image retrieval (CBIR) has been explored by different communities for various applications, such as internet-based information search, data mining in broadcasting archives and improving medical diagnosis.

In the medical domain, there are domain or even modality-specific differences and challenges. The captured images are usually single channel (gray-scale) that differs from multi-channel (e.g. RGB) nature of consumer image and video data. In some medical modalities, such as CT (Computed Tomography), intensity has an absolute scale. In MR, they vary with the scanning parameters, but also with the age of the device and the patient characteristics. To aggravate the problem, the intensity values of a specific tissue may also be non-stationary within a single MR image (a fact known as intensity non-uniformity or bias field) because of imperfect magnetic field and patient-dependent local perturbations. Furthermore, the characteristics of relevant and irrelevant segments of the data are very similar to each other for the databases that are specific to a modality and organ, such as brain MRI data.

To the best of our knowledge, CBIR-based state-of-the-art consists of diagnostic support systems that either exploit generic image retrieval approaches [7], [8], or require expert's feedback to learn inter-subject similarities [1].

In differentiating dementia patients from cognitively normal subjects using image data, visual interpretation is the common practice in the clinical settings [10]. The drawback of qualitative assessment is its large inter-rater variability (mean overall kappa scores measured as high as 0.34) [20]. To overcome this problem of subjectivity, researchers focused on quantitative interpretations of images by employing region-of-interest (ROI) based approaches [2], and voxel-based morphometry (VBM) methods [22]. Due to the spatial limitation of ROI-based approaches and the sensitivity of VBM-based methods to systematic shape differences attributable to misregistration, recent focus has shifted to the use of machine learning methods, such as the discriminant analysis [6] and support vector machines [11, 23, 9].

Machine learning methods are capable of providing more specialized and more accurate solutions, provided that their parameters are optimized for a specific task and dataset. Unfortunately, any change in their task definition or the database, requires re-tuning of their parameters(or re-training). Nevertheless, the promising nature of machine learning methods has been the decisive factor for us to propose a dementia diagnosis solution by combining clinical and patient-related observations with visual features in a machine learning framework. Please note that, reformulation of our proposal in a search and retrieval framework can be achieved by performing similarity comparison between a query and a set of images based on weighted feature combinations, and reaching to a diagnostic decision from the similarity results.

3. METHODOLOGY

In this work we tackle the problem of dementia diagnosis by combining visual attributes computed from longitudinal imaging data with clinical and patient-related information, and making diagnostic decisions based on machine learning. Corresponding data processing steps are illustrated in Figure 1, and further detailed in the following subsections.

3.1 Subjects and Image Data

The data set used in this study consists of a longitudinal collection of 150 subjects, who are suspected to have dementia [13]. Each subject was scanned on two or more visits, separated by at least one year. For each scanning session, 3-4 individual T1-weighted MRI scans were obtained with voxel size 1mm$\times$ 1mm$\times$ 1.25mm, 128 sagittal slices, and matrix dimensions 256$\times$256. Furthermore, whole brain volume (nWBV) and total intracranial volume (eTIV) are automatically calculated and provided with the data set as well.

The screening process included patient information and MR acquisition, as well as two tests to assess the cognitive performance of the subjects: the mini-mental state examination (MMSE) [5] and the clinical dementia rating (CDR) scale [15]. MMSE is a brief commonly used questionnaire, where a score over 27 (out of 30) is effectively normal, while lower scores increasingly correlate with presence of dementia. CDR is a more elaborate, but time-consuming test credited with being able to discern very mild dementia. A CDR score of 0 indicates no dementia, while higher scores show dementia with increasing severity.

Table 1 displays the demographics of the subjects, who come from both genders and have age range of 60-98. Following the screening process, experts characterized 72 subjects as nondemented, 14 as converters, and 64 as demented, where the latter includes 51 individuals with mild to moderate Alzheimer's disease.

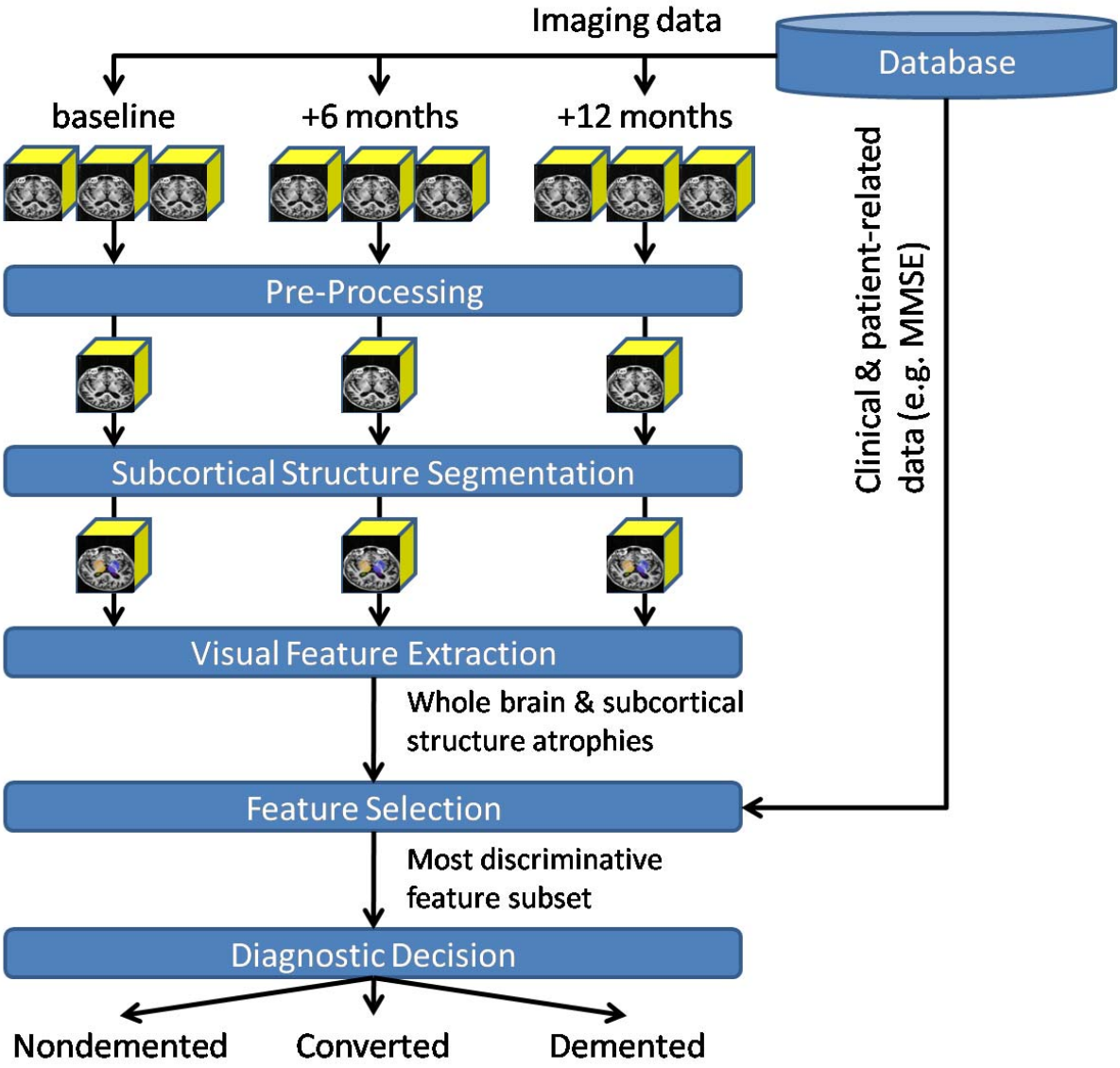

Figure 1: Illustration outlining the processing steps employed.

Table 1: Demographic information on the database.

	NonDemented	Converted	Demented
Sex (F/M)	50/22	10/4	28/36
Age (mean, range)	77.1 (60-97)	79.8 (65-92)	76.3 (61-98)
MMSE score (mean, range)	29.2 (26-30)	28.7 (24-30)	24.2 (0-30)
CDR score (mean, range)	0.01 (0-0.5)	0.26 (0-0.5)	0.67 (0.5-2.0)

F=Female; M=Male; MMSE=Folstein Mini Mental State Examination; CDR=Clinical Dementia Rating.

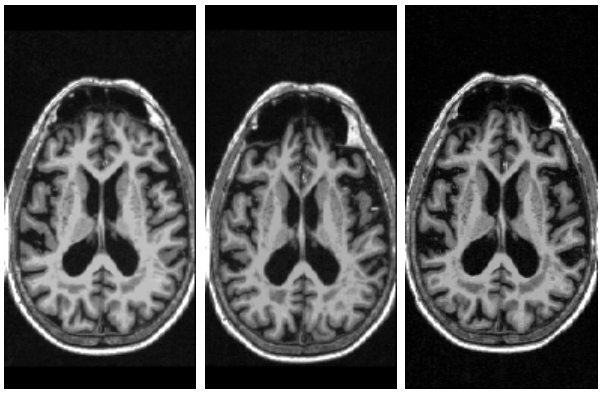

Figure 2: Example pre-processed images of a nondemented subject corresponding to the baseline (left) and two successive follow-up scans.

3.2 Pre-Processing

As the data set contains 3 to 4 individual acquisitions for each scanning session; one needs to create a single image with high contrast-to-noise ratio from these multiple within-session acquisitions using motion-correction and averaging. Moreover, resulting images needed to be intensity normalized and bias field corrected. To this end, we used the FreeSurfer v4.5.0 software package [3]. Figure 2 displays exemplary pre-processed images of a subject from the database.

3.3 Anatomical Structure Segmentation

Segmentation of the subcortical structures in the brain are performed using FIRST (FMRIB's Integrated Registration and Segmentation Tool) v1.2 [16] provided by Oxford Centre for Functional MRI of the Brain (FMRIB). FIRST is a tool for automated segmentation and labeling of the following subcortical structures: brainstem, bilateral amygdala, caudate nucleus, hippocampus, lateral ventricles, nucleus accumbens, putamen, pallidum, thalamus. FIRST comes as a tool already trained on 317 expert labeled T1-weighted MRIs of the brain, from which it learned shape and appearance models based on multivariate Gaussian assumptions. When structures of a T1-weighted MR image is to be segmented, FIRST searches through linear combinations of shape modes of variation from the learned models to find the most probable shape instance in the given image. Examples of automated structure segmentation performed by FIRST are presented in Figure 3.

3.4 Visual Feature Extraction

Late-stage findings of dementia generally include cerebral atrophy and ventricular enlargement, among other observations (e.g. white matter hyperintensities) [14]. Note that cerebral atrophy is defined as loss of neurons, and it is therefore observed as gradual loss (shrinkage) of brain volume. To this end, in this study we decided to use whole brain and subcortical structure atrophies computed from the segmentations as visual features.

Atrophy features are computed by taking the volumetric difference between the baseline and first follow-up scans, and normalizing the differences such that they fall in the [0,1] range:

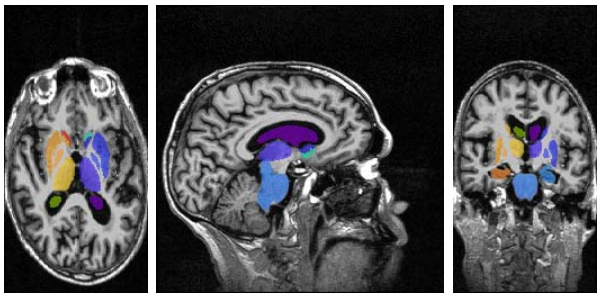

Figure 3: Structure segmentation result of FIRST superimposed on a subject's MRI and displayed from axial (left), sagittal, and coronal (right) views.

$$f_i = |f_i^2 - f_i^1| \tag{1}$$

$$nf_i = \frac{f_i - min(f_i)}{max(f_i) - min(f_i)} \tag{2}$$

where f_i^j refers to the i^{th} feature value computed from the j^{th} scan with $j = 1$ being the baseline acquisition, nf_i is i^{th} normalized feature, and $min(\cdot)$ $max(\cdot)$ operations are computed among all subjects.

Table 2 presents the visual features computed from MRI scans, and the features related to cognitive assessments and patient demographics used in this study.

3.5 Feature Selection

In real-world problems, irrelevant or redundant features may have negative effect on accuracy of a classifier (curse of dimensionality [1]). In order to identify relevant feature subsets, we propose to use sequential floating forward selection method [17]. The algorithm starts with an empty feature subset. At each iteration, it tentatively adds to the feature subset one feature that is not already selected and tests the accuracy of classifier built on the tentative feature subset. The feature that results in the lowest classification error is definitely added to the subset. After each addition step the algorithm removes any previously added feature if its removal decreases error. The process stops after a certain number of iterations (which equals number of features for our case) provided by the user.

3.6 Diagnostic Decision

Diagnostic decision based on the features extracted in the preceeding section is accomplished using a classification approach. Assuming that samples are linearly separable, for the binary case a Linear Discriminant Classifier (LDC) tries to find a linear decision boundary that separates the feature space into two half-spaces by minimizing the following criterion function

$$g(x) = w_0 + \sum_{i=1}^{d} w_i x_i \tag{3}$$

where the coefficients w_i are the components of d-dimensional weight vector w, and x_i is the i^{th} feature value of d-dimensional feature vector x. In this study, Matlab built-in libraries are used for LDC.

[1]Exponential growth of volume as a function of dimensionality of a (mathematical) space

Table 2: Visual, as well as clinical and patient-related features employed in this study.

Type	Acronym	Name
clinical and patient-related features	CDR	Clinical Dementia Rating
	MMSE	Mini-Mental State Examination
	Age	-
	Educ.	Education
	SES	Socio-Economic Status
visual features	eTIV	Total Intracranial Volume
	nWBV	Whole Brain Volume
	LV	Lateral Ventricle
	TP	Thalamus Proper
	CN	Caudate Nucleus
	Put	Putamen
	Pal	Pallidum
	BSt	Brainstem
	Hip	Hippocampus
	Amy	Amygdala
	Acc	Nucleus Accumbens

3.7 Performance Evaluation

Performance evaluation is measured using 10-fold cross validation, where the database is partitioned into ten subsets. Each subset is used once for testing while the rest are used for training, and the final result is assigned as the average of ten validations. Note that for each validation all classes were equally divided among the folds. Overall classification performance is measured using accuracy, which is the number of correct diagnoses divided by the total number of subjects.

4. EXPERIMENTAL RESULTS

4.1 Correlation Analysis

Table 3 presents pairwise linear correlations between each feature and expert diagnoses of the data (ground truth). As dementia is directly related to cognitive abilities, CDR and MMSE that assess cognitive performance of subjects show the strongest correlations with expert diagnoses. CDR, being a more elaborate test, depicts the highest correlation score. Whole brain volume (nWBV), hippocampus (Hip), and Amygdala (Amy) features demonstrate weak correlations, while scores from others are generally not reliable.

4.2 Single Feature Performances

At this point, each feature is input to the classifier individually and their diagnosis accuracies are observed. From this analysis only CDR and MMSE features are found discriminative enough to be reported here. Their respective accuracies are observed as 68.8% and 61.8%.

4.3 Performances of Feature Combinations

Subsequently, CDR and MMSE are disjointly combined and augmented by the visual features proposed in an iterative fashion using the feature selection method. Figures 4 and 5 expose these results in a graphical representation. In the figures, combination of features for each feature selection step (until and including the step with the highest accuracy) along with the highest accuracy value are shown as well.

Figure 4 reveals that augmenting CDR with six visual features (Hip, Amy, Acc, nWBV, Put, BSt) leads to a striking 84% accuracy level, which corresponds to a 22% improvement over the individual performance of CDR.

Although less emphasized, similar observations hold true for the MMSE case as well (Figure 5). Note that augmenting MMSE with all visual features slightly degrades accuracy with respect to the individual performance of MMSE.

Table 3: Correlation scores of each feature with expert diagnoses. *refers to values that are statistically significant at the 5% level.

Feature	Absolute Score
CDR	0.84^*
MMSE	0.56^*
Age	0.04
Educ.	0.24^*
SES	0.00
eTIV	0.03
nWBV	0.31^*
LV	0.07
TP	0.15^*
CN	0.17^*
Put	0.24^*
Pal	0.06
BSt	0.04
Hip	0.38^*
Amy	0.30^*
Acc	0.23^*

4.4 Importance of Visual Features

In order to find out relative importance of visual features in dementia diagnosis, we repeated the above feature selection based analysis hundred times, recorded best performances of each run, and analyzed the recordings to figure out the frequency of observing each visual feature.

Figure 6 presents the results corresponding to the CDR case. Hippocampus, amygdala, and accumbens constitute the top three frequently observed features, followed by putamen and whole brain volume. Notice that these observations are consistent with the best feature combination case illustrated in Figure 4.

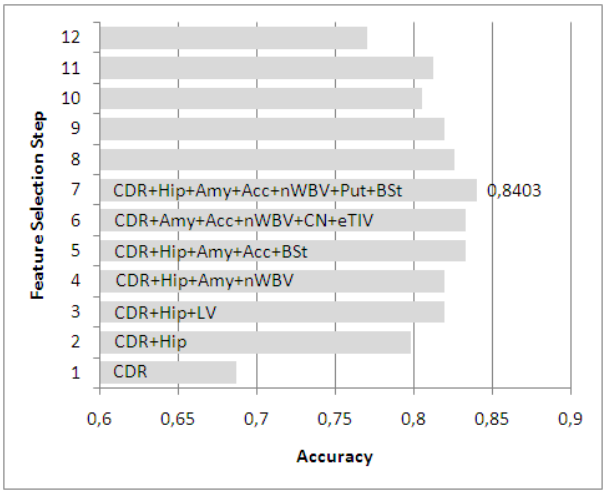

Figure 4: Classification performance observed through iterative combination of visual features with CDR using feature selection.

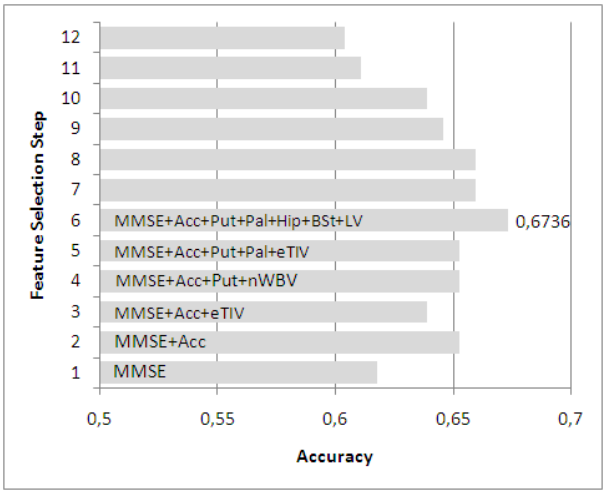

Figure 5: Classification performance observed through iterative combination of visual features with MMSE using feature selection.

Figure 7 demonstrates the results for the MMSE case, where accumbens, lateral ventricle and whole brain volume are observed as the most frequent features, followed by pallidum, brainstem, hippocampus and putamen. Again, most of these visual features are observed in the best feature combination case of Figure 5, as well.

Researchers have been looking for biomarkers for diagnosing dementias from structural MRI and recent findings reveal correlation between atrophy patterns in the temporal lobe (including hippocampus) and cognitive performance, and thus dementia [14]. Accordingly, our observations over important visual features are consistent with the related literature.

4.5 Confusion Matrix of the Best Diagnosis

Table 4 presents the confusion matrix of the best diagnosis accuracy (84%) achieved by the proposed method. Highest accuracy is observed for the nondemented group, whereas diagnosis of demented subjects reaches to 76% accuracy and all confusions are with the 'converted' class. Lowest accuracy, and therefore highest confusion, is observed for the 'converted' group, due to the high difficulty of discriminating subjects of this transition class from others.

Table 4: Confusion matrix of the best diagnosis achieved with the proposed approach. Values in parenthesis refer to ratios within the true class.

	True Class		
	Nondemented	Converted	Demented
Nondemented	68 (.97)	4 (.33)	0 (0)
Converted	1 (.01)	6 (.50)	15 (.24)
Demented	1 (.01)	2 (.17)	47 (.76)

5. CONCLUSION

This paper introduced a novel work on fusing clinical and patient-related features with visual features extracted from longitudinal MRI data for a more accurate dementia diagnosis. Image data were automatically processed to segment several subcortical structures of the brain. Volumetric differences of structures between baseline and follow-up scans were assigned as visual features, which were used together with (especially) cognitive scores in a classification framework for dementia diagnosis. Observations showed that augmenting cognitive scores with a subset of visual features resulted in more accurate predictions. Furthermore, repeating the feature selection process many times and analyzing the results revealed that visual features of some structures are more frequently observed than others, and these structures are generally consistent with the ones that are/were under investigation in the literature.

A straightforward extension of this work is to analyze the effect of incorporating several time-points available in the data, instead of using only baseline and first follow-up scans.

Even though the problem of diagnosing dementia is addressed using a classification framework in this work, one can easily reformulate it as a search and retrieval problem: weighted combination of several features will define an N-dimensional space, where similarities of database items can be computed and decisions can be taken based on most similar items. Accordingly, one future work is to re-attack this problem from a search and retrieval perspective, and perform an in-depth comparison of the two perspectives.

6. ACKNOWLEDGMENTS

The author would like to thank Dr. Ahmet Ekin from Philips Research Europe for the fruitful discussions, and Prof. Aytul Ercil from Sabanci University for her continuous encouragement.

7. REFERENCES

[1] C. B. Akgül, D. Ünay, and A. Ekin. Automated diagnosis of alzheimer's disease using image similarity and user feedback. In *CIVR '09: Proceeding of the ACM International Conference on Image and Video Retrieval*, pages 1–8, New York, NY, USA, 2009. ACM.

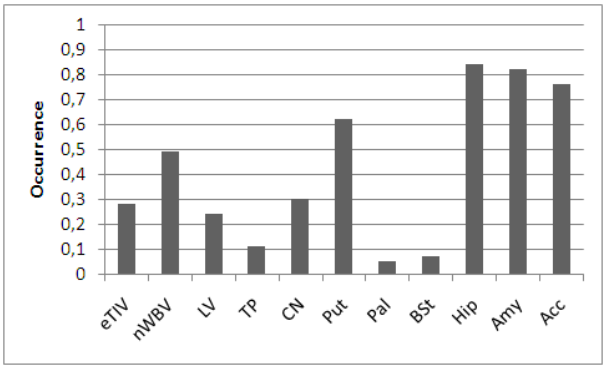

Figure 6: Frequency of observing each visual feature with CDR in the best classification case.

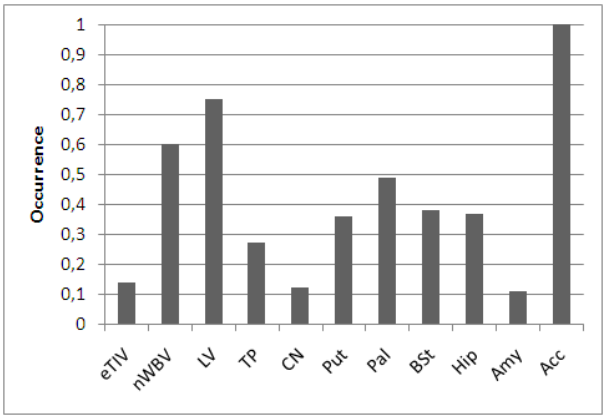

Figure 7: Frequency of observing each visual feature with MMSE in the best classification case.

[2] J. Barnes, R. I. Scahill, R. G. Boyes, C. Frost, E. B. Lewis, C. L. Rossor, M. N. Rossor, and N. C. Fox. Differentiating AD from aging using semiautomated measurement of hippocampal atrophy rates. *NeuroImage*, 23:574–581, 2004.

[3] A. M. Dale, B. Fischl, and M. I. Sereno. Cortical surface-based analysis: I. segmentation and surface reconstruction. *NeuroImage*, 9(2):179 – 194, 1999.

[4] C. P. Ferri, M. Prince, C. Bryne, H. Brodaty, L. Fratiglioni, M. Ganguli, K. Hall, K. Hasegawa, H. Hendrie, Y. Huang, A. Jorm, C. Mathers, P. R. Menezes, E. Rimmer, M. Scazufca, and for Alzheimer's Disease International. Global prevalence of dementia: a delphi consensus study. *Lancet*, 366:2112–17, December 2005.

[5] M. F. Folstein, S. E. Folstein, and P. R. McHugh. "Mini-mental state". A practical method for grading the cognitive state of patients for the clinician. *Journal of Psychiatric Research*, 12(3):189–198, November 1975.

[6] P. A. Freeborough and N. C. Fox. MR image texture analysis applied to the diagnosis and tracking of alzheimer's disease. *IEEE Transactions on Medical Imaging*, 17(3):475–479, 1998.

[7] C.-C. Hsu, W. W. Chu, and R. K. Taira. A knowledge-based approach for retrieving images by content. *IEEE Transactions on Knowledge and Data Engineering*, 8(4):522–532, 1996.

[8] H. K. Huang, J. F. Nielsen, M. D. Nelson, and L. Lui. Image-matching as a medical diagnostic support (DST) for brain diseases in children. *Computerized Medical Imaging and Graphics*, 29(2-3):195–202, 2005.

[9] S. Klöppel, C. M. Stonnington, C. Chu, B. Draganski, R. I. Scahill, J. D. Rohrer, N. C. Fox, C. R. Jack, J. Ashburner, and R. S. J. Frackowiak. Automatic classification of MR scans in alzheimer's disease. *Brain*, 131:681–689, 2008.

[10] D. S. Knopman, S. T. DeKosky, J. L. Cummings, H. Chui, J. Corey-Bloom, N. Relkin, G. W. Small, B. Miller, and J. C. Stevens. Practice parameter: Diagnosis of dementia (an evidence-based review): Report of the Quality Standards Subcommittee of the American Academy of Neurology. *Neurology*, 56(9):1143–1153, 2001.

[11] Z. Lao, D. Shen, Z. Xue, B. Karacali, S. M. Resnick, and C. Davatzikos. Morphological classification of brains via high-dimensional shape transformations and machine learning methods. *NeuroImage*, 21:46–57, 2004.

[12] M. S. Lew, N. Sebe, C. Djerba, and R. Jain. Content-based multimedia information retrieval: state of the art and challenges. *ACM Transactions on Multimedia Computing, Communications, and Applications*, 2(1):1–19, Feb. 2006.

[13] D. S. Marcus, T. H. Wang, J. Parker, J. G. Csernansky, J. C. Morris, and R. L. Buckner. Open access series of imaging studies (OASIS): Cross-sectional MRI data in young, middle aged, nondemented, and demented older adults. *Journal of Cognitive Neuroscience*, 19(9):1498–1507, 2007.

[14] B. L. Miller. Past Glory and Future Promise: Maximizing and Improving Understanding of Atrophy Patterns in the Diagnosis of Degenerative Dementias. *American Journal of Neuroradiology*, 23(1):33–34, 2002.

[15] J. C. Morris. The clinical dementia rating (CDR): current version and scoring rules. *Neurology*, 43:2412–2414, 1993.

[16] [online]. http://www.fmrib.ox.ac.uk/fsl/.

[17] P. Pudil, F. J. Ferri, J. Novovicova, and J. Kittler. Floating search methods for feature selection with nonmonotonic criterion functions. In *In Proceedings of the Twelveth International Conference on Pattern Recognition, IAPR*, pages 279–283, 1994.

[18] Y. Rui, T. Huang, and S. Chang. Image retrieval: current techniques, promising directions and open issues. *Journal of Visual Communication and Image Representation*, 10(4):39–62, Apr. 1999.

[19] P. Scheltens, N. Fox, F. Barkhof, and C. De Carli. Structural magnetic resonance imaging in the practical assessment of dementia: beyond exclusion. *Lancet Neurology*, 1:13–21, 2002.

[20] P. Scheltens, F. Pasquier, J. G. E. Weerts, F. Barkhof, and D. Leys. Qualitative assessment of cerebral atrophy on MRI: Inter- and intra-observer reproducibility in dementia and normal aging. *European Neurology*, 37(2):95–99, 1997.

[21] D. H. S. Silverman, G. W. Small, and M. E. Phelps. Clinical value of neuroimaging in the diagnosis of dementia: Sensitivity and specificity of regional cerebral metabolic and other parameters for early identification of alzheimer's disease. *Clinical Positron Imaging*, 2(3):119–130, 1999.

[22] P. M. Thompson, K. M. Hayashi, R. A. Dutton, M. C. Chiang, A. D. Leow, E. R. Sowell, G. De Zubicaray, J. T. Becker, O. L. Lopez, H. J. Aizenstein, and A. W. Toga. Tracking alzheimer's disease. *Annals of the New York Academy of Sciences*, 1097:183–214, February 2007.

[23] P. Vemuri, J. L. Gunter, M. L. Senjem, J. L. Whitwell, K. Kantarci, D. S. Knopman, B. F. Boeve, R. C. Petersen, and C. R. Jack. Alzheimer's disease diagnosis in individual subjects using structural mr images: validation studies. *NeuroImage*, 39:1186–1197, 2008.

[24] G. Waldemar, B. Dubois, M. Emre, P. Scheltens, P. Tariska, and M. Rossor. Diagnosis and management of alzheimer's disease and other disorders associated with dementia. the role of neurologists in europe. *European Journal of Neurology*, 7:133–144, 2000.